V-Doped Starch/Graphitic-Carbon Nitride Composite for Enhanced Pollution Degradation through Response Surface Methodology: The Study of Photocatalytic and Adsorption Process

Chegeni, Mahdieh[*][+]*; Soleymani, Mousa; Eftekhari, Noushin*
Department of Chemistry, Ayatollah Boroujerdi University, Boroujerd, I.R. IRAN

ABSTRACT: *The V-doped starch/graphitic carbon nitride was synthesized for the degradation of organic pollutants. This novel photocatalyst was characterized by various techniques including Fourier Transform InfraRed (FT-IR) spectroscopy, Field Emission Scanning Electron Microscopy (FESEM), X-ray Diffractometer (XRD), Photoluminescence (PL) spectroscopy, Energy Dispersive X-ray (EDX), Transmission Electron Microscopy (TEM), and Brunauer-Emmett-Teller (BET) analysis. Based on the Central Composite Designs-Response Surface Methodology (CCD-RSM) design, 50 full experiments were done including pH (7.8-9.8), adsorbent dose (0.01-0.1 g), MB concentration (2-12 ppm), time (30-240 min), and temperature (15-45 °C) for the methylene blue removal by V-doped starch/graphitic carbon nitride, and the best removal yield (90.8 %) was obtained at pH=8.33, 0.08 g adsorbent dose, 12 ppm of MB concentration, 215 min, and 15 °C. Further, the interaction of adsorption parameters was considered, and the Freundlich and pseudo-second-order were shown as the best adsorption models. After the adsorption process, the photocatalytic degradation of MB was conducted under UV irradiation with high yield (92 %), and the trapping experiments confirmed the photocatalytic degradation. As a result, the V-doped starch/graphitic carbon nitride can be employed for the adsorption and photocatalytic activities for the removal of organic pollutants from aqueous solution.*

KEYWORDS: *Degradation; Graphitic carbon nitride; Photocatalyst; Starch.*

INTRODUCTION

Today, environmental issues are considered an effective and important subject in human life. The exploitation of new technology has attracted scientists to obtain helpful strategies for solving environmental problems [1,2]. One of these clean methods is the photocatalysis strategy, which is applied in many fields such as water treatment [3], and photocatalytic disinfection [4]. A large number of semiconductors have been used as photocatalyst such as TiO_2 [5, 6], bio-magnetically recoverable palladium [3], CeO_2 [7], SnO_2 [8], pure ZnO and MgO doped ZnO nanocatalysts [9], polypyrrole/halloysite nanotubes/Fe_3O_4/Ag/Co nanocomposite [10], and Nd-doped ZnO nanoparticles [11]. Further, the low response forward visible light and self-oxidation can limit photocatalytic performance. Meanwhile,

the construction of novel photocatalysts is a valuable subject, so scientists try to design new structures.

Polymeric graphitic carbon nitride (g-C_3N_4) is considered as a new generation of photocatalyst, because of its properties including chemical and thermal stability, band gap, eco-friendly, and resistance toward chemical compounds [12]. g-C_3N_4 can be obtained by using cheap precursors including carbon and nitrogen such as cyanamide [13], melamine [14], thiourea [15], and urea [16]. In view of g-C_3N_4 application, it can be employed for fuel cells [17], catalysis [18], water splitting [19], antibacterial activity [20], adsorption [21], electrochemical sensor [22], and batteries utilization [23]. Notably, pure g-C_3N_4 can suffer some disadvantages including limitations in the recombination rate of photon-generated carriers and electrical conductivity. For the improvement of g-C_3N_4 properties, several strategies were served such as atom doping [24], morphology modification [25], and the formation of composite [26]. A large number of studies have reported the improvement of g-C_3N_4 properties including metal/graphitic carbon nitride composites [27], clay minerals supported graphitic carbon nitride [28,29], porous carbon/graphitic carbon nitride composites [30]. Further, a surge of interest has been attracted to the use of natural compounds, due to their green and eco-friendly properties. According to reported articles, perovskite [31], RM and bauxite [29], chitosan [32], and perlite [33] were applied to the modification of g-C_3N_4.

To achieve sustainable development, the use of biodegradable polymers is a suitable strategy [34-36]. Several biopolymers were used in different applications such as chitosan-modified Pd(II)-d-penicillamine [37], cross-linked chitosan aerogel modified with Pd(II)/phthalocyanine [38], cellulose-modified with Fe(II)- and Ni(II)–phthalocyanines [39]. With the development of polysaccharide subject, starch is recognized as an eco-friendly and low-cost polymer with the ability of mix with other compounds and more applications in various industries. In addition, the composite formation by using starch is difficult, and the use of fillers was proposed as an important strategy to overcome starch limitations.

Further, V_2O_5 was used as an n-type semiconductor, photo, and chemical stability, which addresses the shortcomings of g-C_3N_4. Numerous studies investigated its photocatalyst activity such as the formation of V_2O_5/Al_2O_3 [40], $V_2O_5/BiVO_4$ composite [41], and ZnO–V_2O_5–WO_3 composites [42].

One of the synthetic pigments is Methylene Blue (MB), which applied in many industries such as silk, paper, wool, and so on. The release of untreated MB dye-loaded wastewater can be resulted in tissue necrosis, cyanosis vomiting growth inhibition, and protein content of microalgae, due to its teratogenic and embryotoxic properties. Various methods are available for the removal of MB such as reverse osmosis, electrolysis, coagulation-flocculation, irradiation, and adsorption. Some of these strategies have some disadvantages including expensive procedures, and the increase of by-products, that can limit their application [43, 44].

The blend of starch/g-C_3N_4 and V_2O_5 can improve their properties, which enhances more application as a photocatalyst. To improve the environmental concerns, this study focused on the formation of a novel composite by using g-C_3N_4 and starch as a polysaccharide, and atom-doping was applied as an interesting protocol to solve the limitation of g-C_3N_4 [45], then the ability of as-synthesized composite for removing MB was studied by adsorption and photocatalytic methods.

To evaluate the effective parameters (pH, MB concentration, composite dose, time, and temperature) for the adsorption process, the optimization step is necessary for finding the best yield. Notably, the Response Surface Methodology (RSM) is used to optimize the experiments by using mathematical techniques such as linear, and quadratic, and it can determine the interaction of parameters, and the costs can be decreased by designing an experiment. Further, Central Composite Designs (CCD) is employed as an attractive model to demonstrate the experimental runs and conditions [46]. Numerous studies explained the removal of pollutants by using RSM method such as pb (II) adsorption onto chitosan-coated Fe_3O_4 particles [47], Eriochrome black-T dye adsorption using modified clay [48], crystal violet with Centaurea stem [49], and dye removal by amine-modified zeolitic imidazolate framework-8 [50].

To achieve the aims of green chemistry, the use of natural materials and the design of sufficient composite can be mentioned for reducing organic pollutants. The high recombination rate of electron-hole pairs can decrease the photocatalytic activity of g-C_3N_4. In order to improve the removal of dye, the modification of g-C_3N_4 was done

by vanadium as a semiconductor and starch for increasing separation of ion-holes pair and photocatalytic performance. Few researchers have addressed the use of natural compounds for the improvement of g-C$_3$N$_4$-based composite, and this research reports the combination of starch as a polysaccharide and g-C$_3$N$_4$ to overcome the limitation of starting materials, then the study reports the synthesis of starch/graphitic carbon nitride (starch/g-C$_3$N$_4$), and as follows doping by vanadium was performed to obtain V-doped starch/g-C$_3$N$_4$ as a novel composite. This study differs from other reports in some reasons such as the study of adsorption and photocatalytic methods for the removal of MB and the use of CCD-RSM strategy for considering the impact and interactions of important factors.

The as-synthesized composite was analyzed by several techniques, and the removal of MB as organic pigments was considered through RSM method, then the effective parameters were relieved including pH (7.8-9.8), MB concentration (2-12 ppm), composite dose (0.01-0.1 g), time (30-240 min), and temperature (15-45 °C), and the isotherm model and kinetic order were studied. After the study of the adsorption procedure, the degradation of MB was investigated under the optimum conditions and Ultraviolet (UV) irradiation. Meanwhile, this work is focused on the application of natural and semiconductor compounds in the photocatalytic subject for the degradation of pollutants.

EXPERIMENTAL SECTION
Materials and instruments

Melamine, methylene blue, sodium hydroxide (NaOH), hydrochloric acid (HCl), starch, and ammonium metavanadate (NH$_4$VO$_3$) were purchased from Merck Co. The morphologies were obtained by Field Emission Scanning Electron Microscopy (FESEM) (TescanMira3-Lmu) and Transmission Electron Microscopy (TEM) (CM120, Poland). The functional groups were characterized by Unicam-Galaxy 5000 FT-IR with KBr pellets, and the Panalytical Xpertpro diffractometer Cu Kα radiation (λ=1.54178 Å) was employed to obtain crystal phase. The Ultraviolet-Visible (UV) spectroscopy (Dynamica–HALO- DB–20, Germany) was used to determine MB amount at λ_{max}=651 nm. The BET isotherm of the V-doped starch/g-C$_3$N$_4$ composite was obtained by Belsorp-Mini II and Bel Prep VAC II (BEL, Japan). PerkinElmer LS-55 fluorescence Spectrometer was used to determine PL properties (λ_{max}=435).

Synthesis of V-doped starch/g-C$_3$N$_4$

For the synthesis of starch/g-C$_3$N$_4$, g-C$_3$N$_4$ was prepared according to Ref [51]. Briefly, 5 g melamine was put into a crucible, and heated until 550 °C for 90 min, then the ratio (1:2) of starch/g-C$_3$N$_4$ was mixed and heated in a crucible at 150° C for 1 h. Second, starch/g-C$_3$N$_4$ and NH$_4$VO$_3$ (2:1) were placed in an alumina crucible at 500° C for 1h. Finally, the V-doped starch/g-C$_3$N$_4$ was obtained (58 % yield), and applied for MB degradation in an aqueous solution.

Experimental design

RSM is used as a common factorial design for the evaluation MB removal, and the removal efficiency (%) was determined by CCD design and Design-Expert 7.0 with 50 runs (Tables 1,2S). The influence of parameters was demonstrated including concentration of MB, dose of photocatalyst, pH, time, and temperature. From the view of pH, the pHpzc (point of zero charge) was determined 7.8. When the pH is higher than 7.8, the yield of removal was increased, because the MB as a cationic due was adsorbed at the negative value of the adsorbent surface. Based on the CCD design, a certain amount of MB and adsorbent were mixed together under determined pH and time, then the mixture was centrifuged and filtered. The MB amount was calculated by the data of absorption at λ_{max}=651 nm. The MB concentration adsorbed at the equilibrium removal percentage (%) was calculated by using Equations 1S-2S, respectively.

Adsorption isotherms and kinetics studies

The Freundlich and Langmuir isotherms were considered to find the adsorption performance by using Equations (3S,4S) and explain the multilayer and monolayer adsorptions [52]. Also, the pseudo-first-order and the pseudo-second-order kinetic models were used to determine adsorption performance, respectively. According to Equations (5S, 6S), the kinetic process of the dye removal is relieved.

Radical species trapping tests

After the adsorption process, the photocatalytic experiment was studied under optimum parameters and dark, 5 W LED lamps (450 nm), and UV (300 W Xe lamp, 345 nm cut-off filter) conditions. The main reactive species involve superoxide (˙O$_2^-$), hydroxyl (˙OH), holes (h$^+$) in the photocatalytic degradation. To find degradation

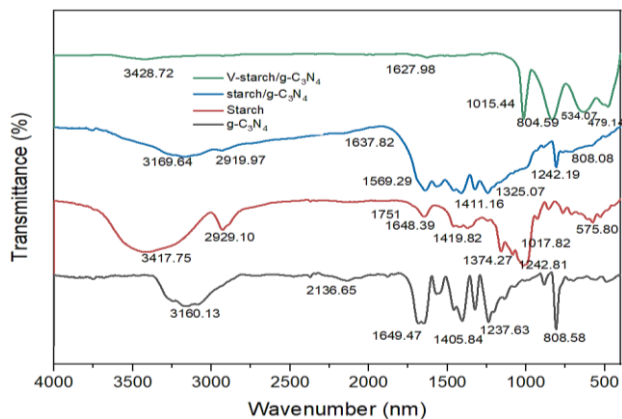*Fig. 1: FT-IR spectra of g-C₃N₄, starch, starch/g-C₃N₄, and V-doped starch/g-C₃N₄.*

Fig. 2: XRD patterns of g-C₃N₄, starch/g-C₃N₄, and V-doped on starch/g-C₃N₄.

mechanism, trapping experiments were done by scavengers such as IPA, hydrazine, and AO to determine h^+, $^{\cdot}O_2^-$ and $^{\cdot}OH$ radicals [18].

After photocatalytic procedure, Total Organic Carbon (TOC) was measured as important factor for analyzing the amount of total organic carbon organic carbon, which carried out by TOC analyzer (CR3200, WTW, Germany), that potassium phthalate solution was used as the calibration standard. The removal percentage was calculated by Equation (1), whereas $[TOC]_o$ and $[TOC]_t$ are the initial and final concentrations of organic compounds.

$$Mineralization \ (\%) = \frac{[TOC]_o - [TOC]_t}{[TOC]_o} \qquad (1)$$

RESULTS AND DISCUSSION

The V-doped starch/g-C₃N₄ was synthesized by a simple method and its formation was characterized by various techniques. The various methods such as ultrasonication and thermal methods were applied and analyzed, then the thermal strategy was chosen for the synthesis of V-doped starch/g-C₃N₄. The functional group of compounds were confirmed by FT-IR spectroscopy, which provides as shown in Fig. 1. Starch FT-IR spectrum is assigned by the peaks at 3100-3500 cm⁻¹, which correspond to stretching vibration of -O-H bond. The peaks at 1751 and 1375 cm⁻¹ are ascribed by stretching vibration of -C=O and C-CH₃ bonds. The stretching vibration of C-O bond is determined between 900-1250 cm⁻¹. In the FT-IR spectrum of g-C₃N₄, the absorption bands at 3100-3500 cm⁻¹ are attributed to the stretching vibrations of –NH₂ or =NH groups. The peaks at 1250 ~1400 cm⁻¹ are corresponded to the stretching modes of
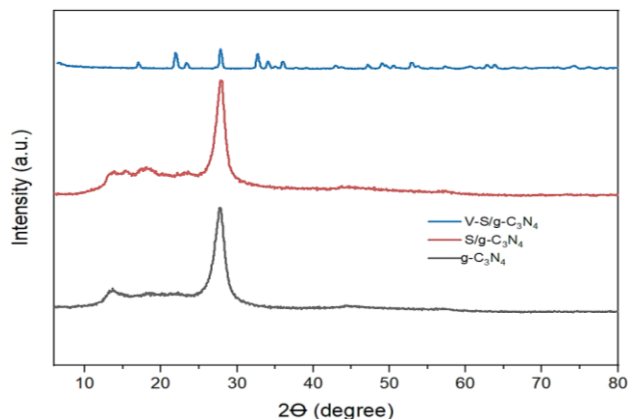
aromatic C-N bonds and the carbon nitride heterocycle is determined by the peak at 808 cm⁻¹. The starch/g-C₃N₄ FT-IR spectrum is shown in Fig. 1, and indicates by the broad peaks at 2800-3500 cm⁻¹, which corresponds to the hydrogenic bond between starch and g-C₃N₄. The absorption bands at 1569-1637 cm⁻¹ are determined to the stretching mode of (C=N), and the peaks at 1242, 1325, and 1411 cm⁻¹ are assigned by aromatic (C-N) bonds, which the C-N heterocycle bond is related to the peak at 808 cm⁻¹. For the V-doped starch/g-C₃N₄, the peaks at 479, 634, and 1015 cm⁻¹ have belonged to the stretching modes of (V=O) bonds, and the bands at 3000-3428 cm⁻¹ are relieved hydrogen bonds among components of composite, which the peak at 808 cm⁻¹ is confirmed the presence of carbon nitride heterocycle.

The X-Ray powder Diffraction (XRD) was carried out to determine the crystal structure of g-C₃N₄, starch/g-C₃N₄, and V-doped starch/g-C₃N₄. Fig. 2 shows the diffraction peaks of g-C₃N₄ at 2Θ =13.3° and 28.2° (JCPDS Card No. 87-1526), that the peaks have corresponded to the heterocycle ring and aromatic plane, which ascribed by (1 0 0) and (0 0 2) crystal faces. As shown in XRD pattern of starch/g-C₃N₄, the peaks at 2Θ 15.2°, 18.4°, 20.2°, and 23.3° are determined A-type crystallite of starch [53], which the presence of g-C₃N₄ peaks can be illustrated the formation of the as-prepared composite. For the XRD pattern of V-doped starch/g-C₃N₄, the peak at 2Θ 27.9° is assigned by graphitic carbon nitride, and the 2Θ 17°, 21.9°, 23.4°, 32.8°, 34°, and 36° are evidenced the presence of starch and V₂O₅ (orthorhombic structure), which the decrease of intensity represents the thin layer thick with 26 nm particle size.
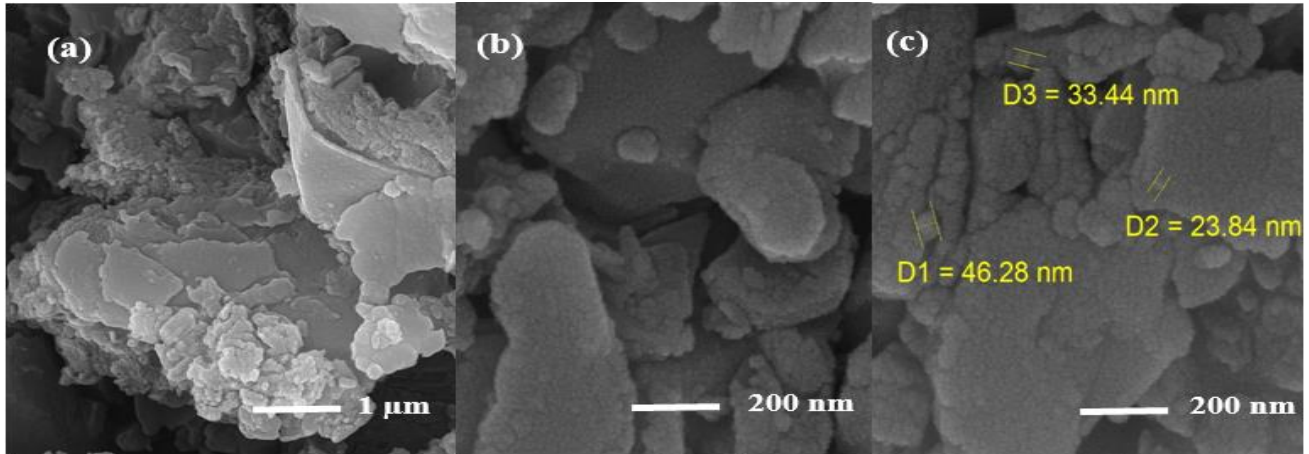
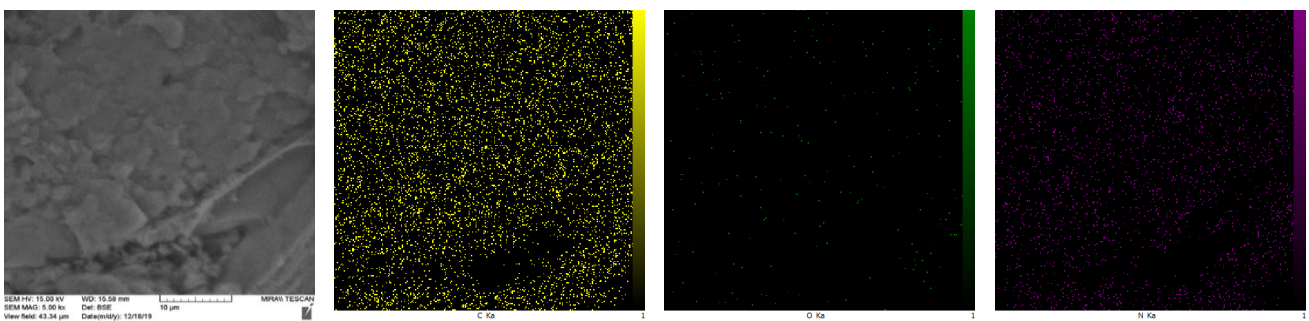*Fig. 3: FESEM images of (a) starch/g-C$_3$N$_4$, (b,c) V-doped starch/g-C$_3$N$_4$.*
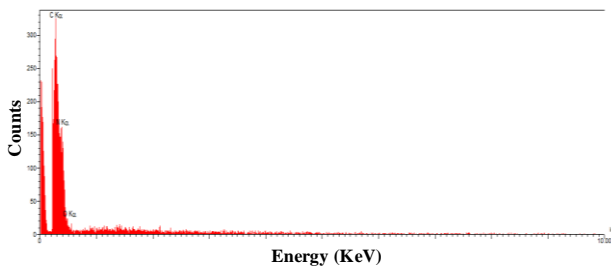

Fig. 4: EDX maps of starch/g-C$_3$N$_4$

Fig. 5: EDX spectrum of starch/g-C$_3$N$_4$

Field Emission Scanning Electronic Microscopy (FESEM) was applied to obtain the morphology of g-C$_3$N$_4$, starch/g-C$_3$N$_4$, and V-doped starch/g-C$_3$N$_4$. Further, the starch/g-C$_3$N$_4$ structure is shown in the layer of g-C$_3$N$_4$ and starch beads, as shown in Fig. 3a. Further, the interaction of starch/g-C$_3$N$_4$ and vanadium particles is shown by the distribution of particles on starch/g-C$_3$N$_4$ surface, in Fig. 3(b,c).

Furthermore, the EDX analysis is shown in Figs. 4 and 5, in which the content of starch/g-C$_3$N$_4$ composite includes C, N, and O elements. The formation of V-doped starch/g-C$_3$N$_4$ is confirmed by Figs. (6-7), which illustrate the presence of C, N, O, and V atoms, which the as-synthesized composite was synthesized uniformly.

As shown in Fig. 8(a-c), TEM images were done to present the morphology of the as-synthesized composite. The g-C$_3$N$_4$ displays wrinkled surfaces and lamellar structure. The images of V-doped starch/g-C$_3$N$_4$ provide a rough surface by comminating g-C$_3$N$_4$ with starch and vanadium. Also, the morphology can be shown amounts of carbon, which was obtained in the thermal process.

In addition, PL spectroscopy was carried out to confirm the photocatalytic activity of the as-prepared composite [3]. As shown in Fig. 9, the peak intensity in V-doped starch/g-C$_3$N$_4$ is weaker than that of g-C$_3$N$_4$. The low PL peak is indicated by the lower charge recombination, so the V-doped starch/g-C$_3$N$_4$ shows appropriate electrical conductivity and good photogenerated hole-electron of the V-doped starch/g-C$_3$N$_4$ composite.

BET analysis was carried out to determine the textural properties of V-doped starch/g-C$_3$N$_4$. The nitrogen adsorption-desorption isotherm curve is shown in Fig. 10, which corresponds to type IV isotherms with H3 hysteresis
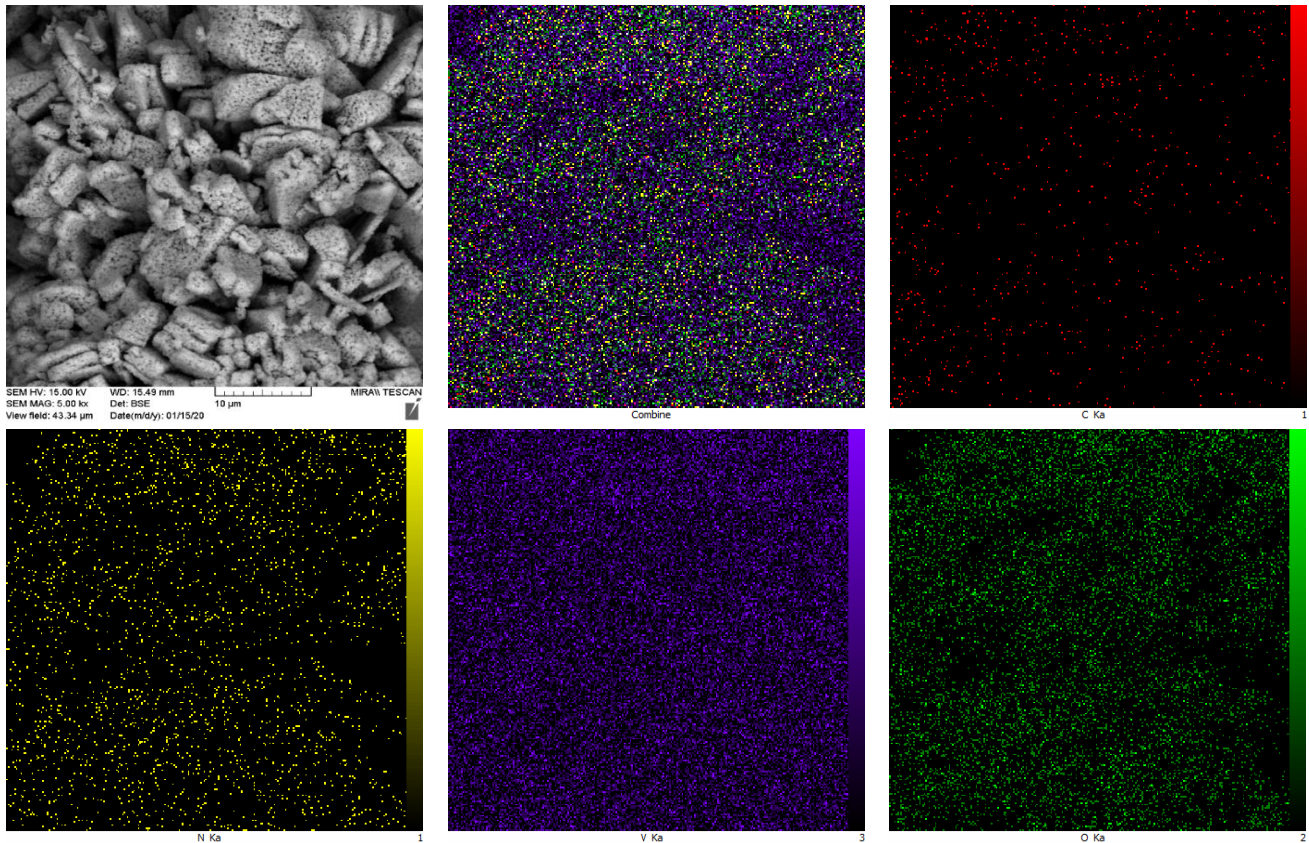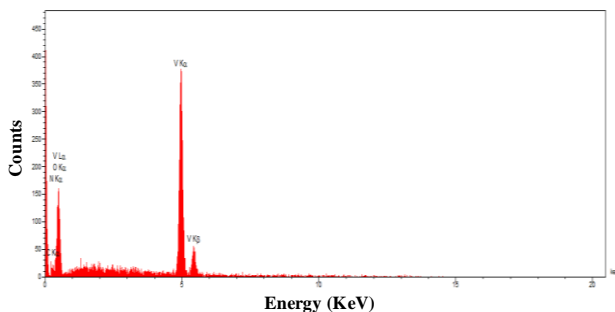
Fig. 6: EDX maps of V-doped starch/g-C$_3$N$_4$.

Fig .7: EDX spectrum of V-doped starch/g-C$_3$N$_4$.

loops. According to the data, the BET surface, total pore volume, mean pore diameter of V-doped starch/g-C$_3$N$_4$ were determined 5.86 m^2/g, 0.016 cm^3/g, and 11.53 nm, respectively. The low BET surface of as-prepared composite was obtained compared to starch/g-C$_3$N$_4$, due to the immobilization and aggregation of particles.

Adsorption and photocatalytic studies

To achieve the best results for the removal of MB as a cationic dye, the important factors of the adsorption process were studied and determined, then the photocatalytic performance was tested under the optimum condition and UV irradiation. Based on the RSM-CCD design, the influence of parameters was evaluated including pH (A), V-doped starch/g-C$_3$N$_4$ dose (B), MB concentration (C), temperature (E), and time (D) (Table 2S). According to the Table 2S, several experiments were done and calculated by Design expert software, and Equation 2 was suggested by software. The removal of MB was achieved to the best result at pH=8.33, 0.08 g adsorbent dose, 12 ppm of MB concentration, 215 min, and 15 °C.

$$
\begin{aligned}
\text{Removal} = &+ 89.34 - 2.27 * A + 4.29 * B + 11.81 \\
&* C + 0.49 * D - 3.95 * E + 1.47 * A * B + 2.40 * \\
&A * C + 1.99 * A * D - 0.68 * A * E + 1.51 * B * \\
&C - 0.16 * B * D + 1.18 * B * E + 1.84 * C * D + \\
&3.26 * C * E - 2.73 * D * E - 0.66 * A^2 - 3.84 * \\
&B^2 - 5.54 * C^2 - 1.96 * D^2 - 0.069 * E^2
\end{aligned}
\tag{2}
$$

Based on the data, the quadratic model was selected as a sufficient model, due to the value of p was less than 0.05. Further, the predicted R^2 (0.9855) has corresponded to the adjusted R^2 (0.4907), and the Adeq Precision was obtained 8.048 as a suitable design model. Furthermore, the high
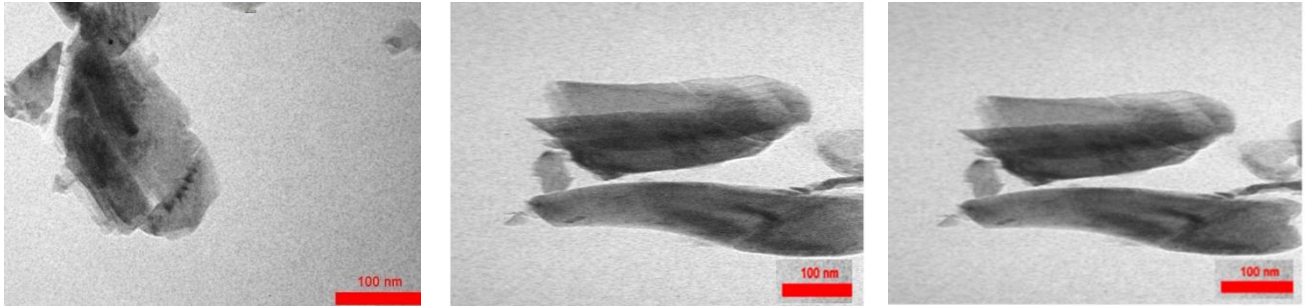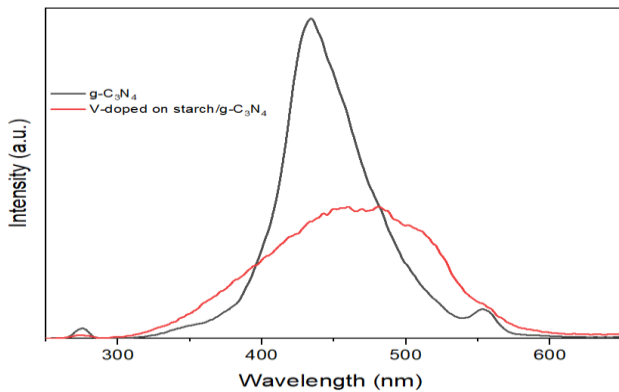
Fig. 8: TEM images of V-doped starch/g-C₃N₄

Fig. 9: PL spectra of g-C₃N₄ and V-doped starch/g-C₃N₄.
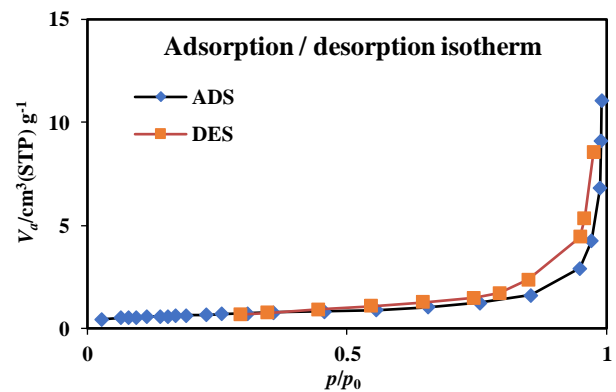

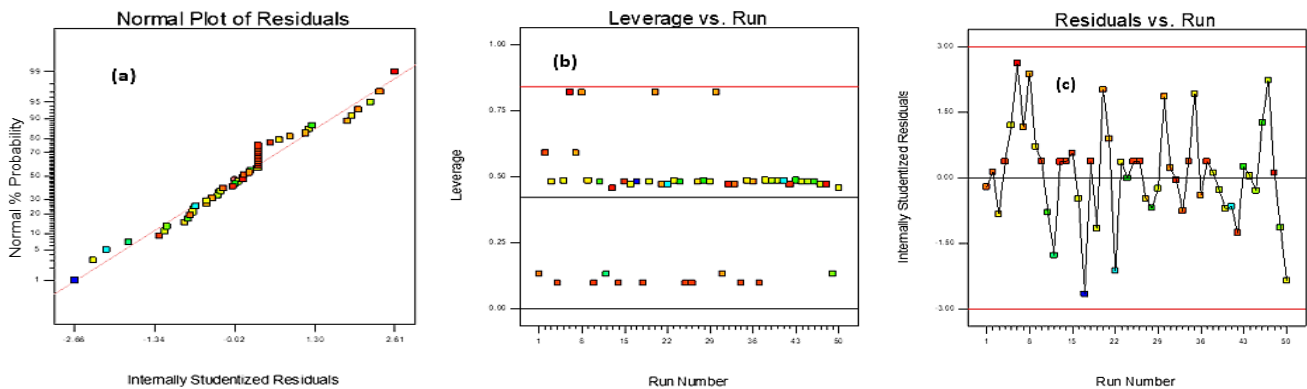*Fig. 10: BET curve of V-doped starch/g-C₃N₄.*

Fig. 11: RSM diagnostic plots for (a) Normal plot of residual (b) Leverage vs Run, and (c) Residuals vs. Run for the MB adsorption by V-doped starch/g-C₃N₄ composite.

effect on the performance of MB removal was shown as follows V-doped starch/g-C₃N₄ dose>pH>temperature>MB concentration>time. The quadratic method was shown the suitable model by corresponding between the experimental and predicted values (residual) without clustering, as shown in Fig. 11(a-c). In Fig. 12(a,b), the interaction between pH and V-doped starch/g-C₃N₄ amount is shown at midpoints of 27 °C and 200 min, and MB was adsorbed on the negative surface at high pH. By increasing the surface of V-doped on starch/g-C₃N₄, the amount of MB

adsorbed was increased (Fig. 12c). The Fig. 12d provides the relation of MB concentration and temperature, which represents the positive influence of these factors at pH=8, 0.08 g of adsorbent, and 197 min (Fig. 12d).

Adsorption isotherm and kinetic studies

For the description of the adsorption mechanism, the Langmuir and Freundlich models were used to explain the performance of MB removal. According to Langmuir and Freundlich model (Fig. 13), the curve of isotherm models

Table 1: Langmuir and Freundlich adsorption isotherm parameters for MB removal by V-doped on starch/g-C₃N₄.

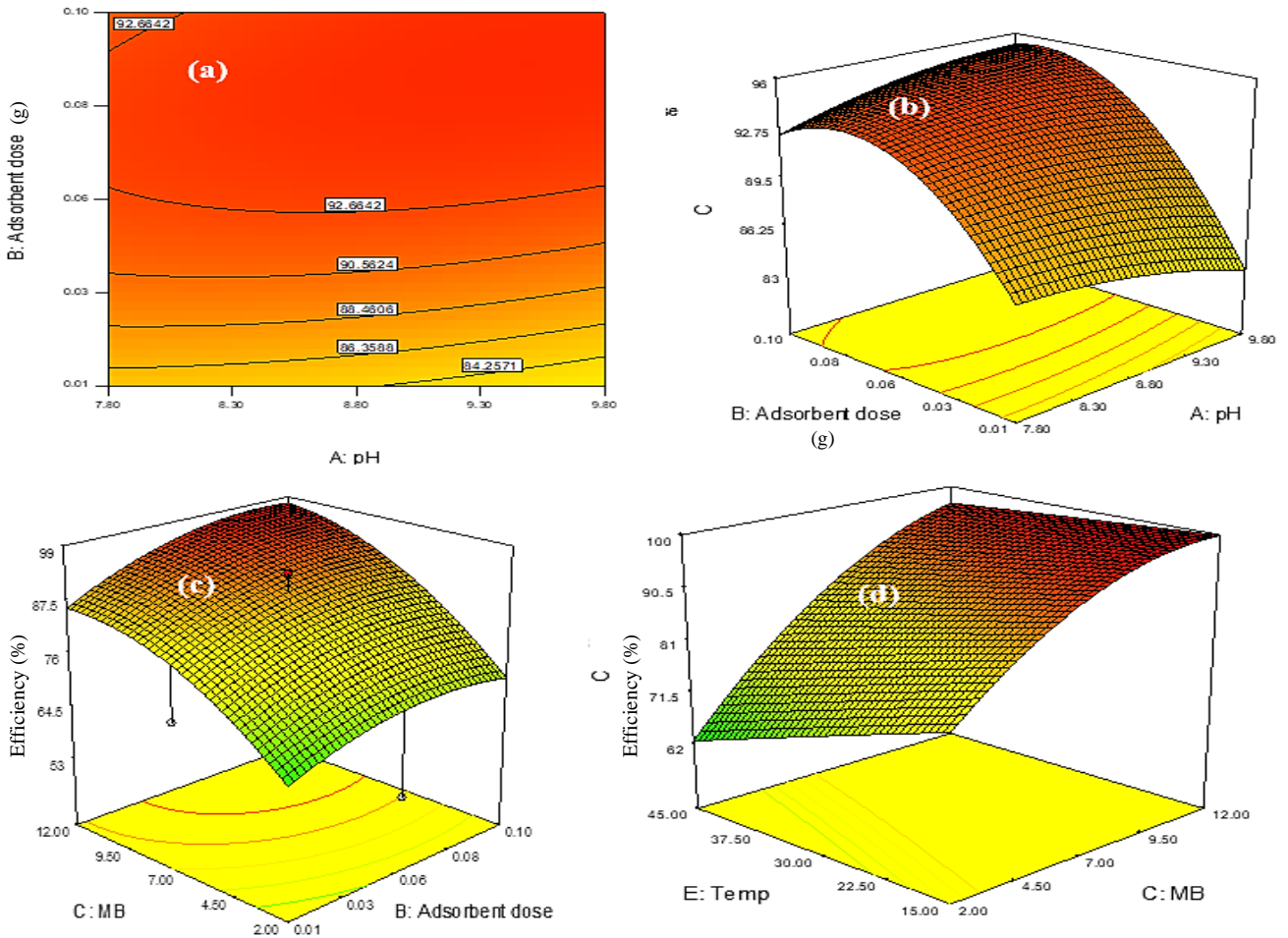| Adsorbent	Langmuir isotherm			Freundlich isotherm		
	K_F (mg/g) (mg/L)^2	n	R^2	q_{max} (mg/g)	b (mg/L)	R^2
MB	0.34	3.29	0.73	4.3	0.07	0.93

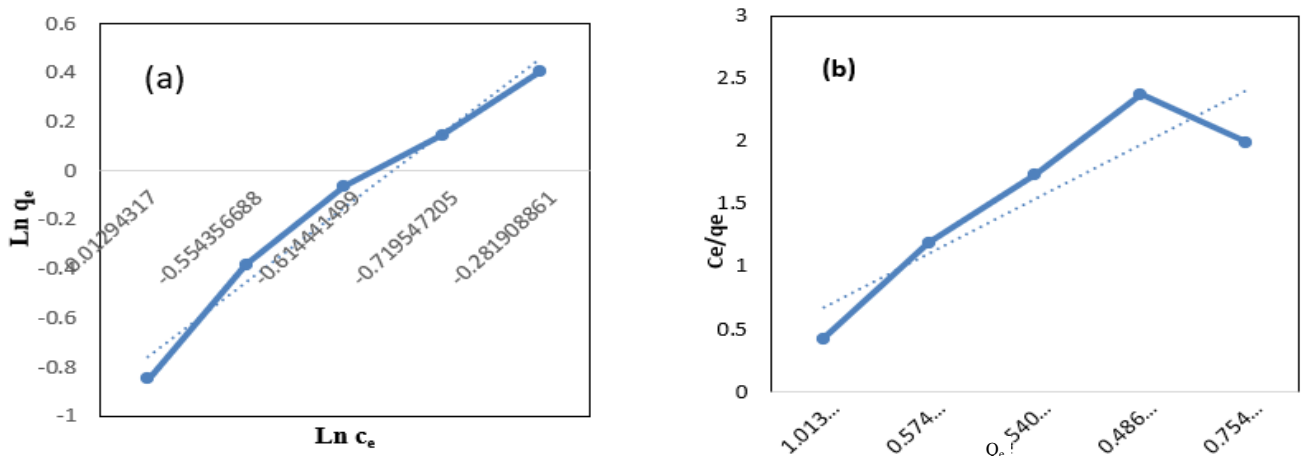*Fig. 12: Response level diagram of the MB removal by V-doped starch/g-C₃N₄.*

Fig. 13: Freundlich and Langmuir isotherms of MB removal by V-doped starch/g-C₃N₄.
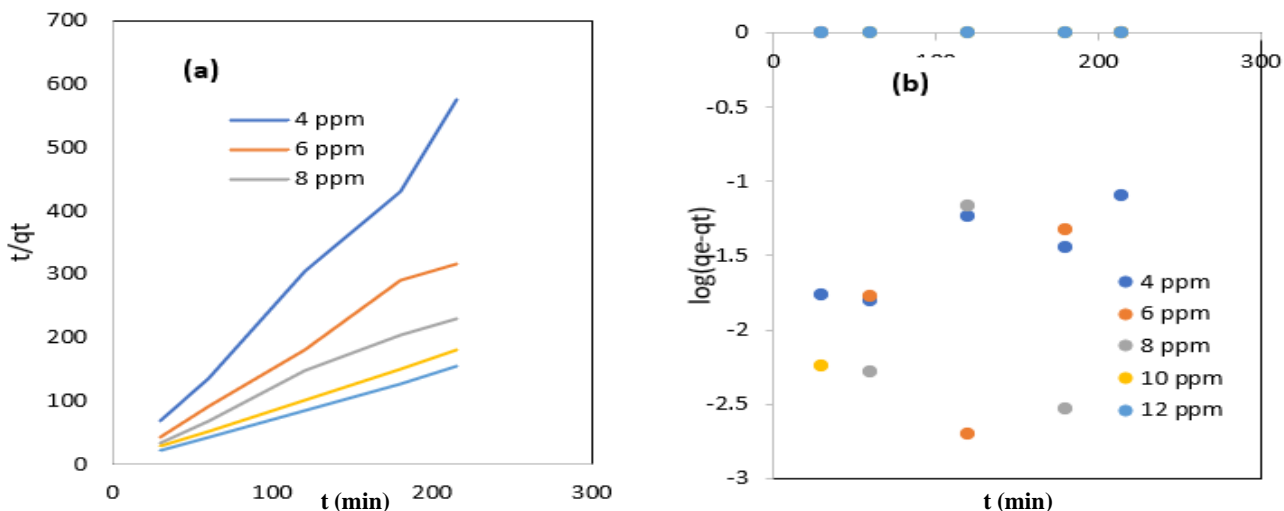
Fig. 14: (a) pseudo-second order, and (b) Pseudo-first order kinetic model diagrams for MB adsorption by V-doped starch/g-C₃N₄.
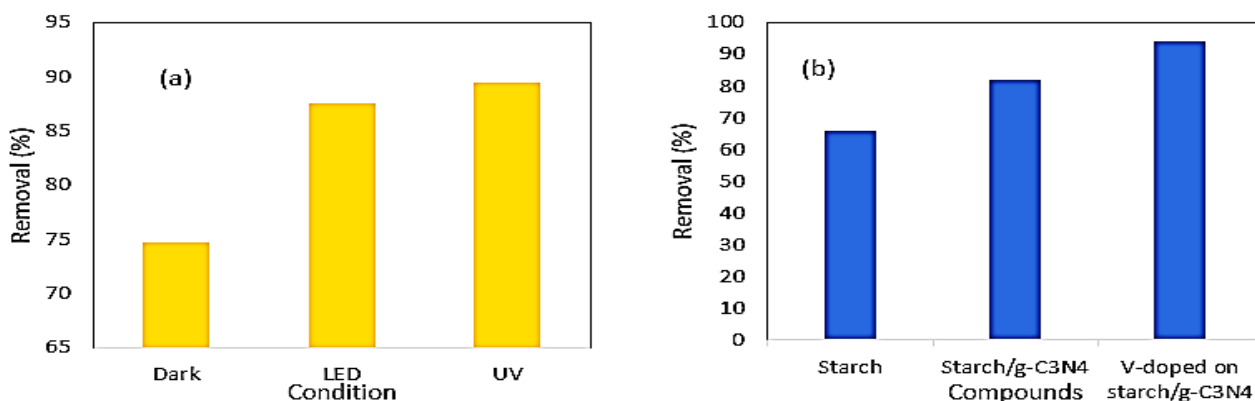

Fig. 15: Efficiency of MB removal by various (a) condition, (b) compounds.

was plotted by Ln qe versus LnCe and Ce/qe versus Ce. Based on Table 1, the Freundlich model was corresponded to the MB removal, due to the high value of regression coefficient (R^2=0.93), and the pseudo-second-order kinetic model corresponded for the MB adsorption by V-doped starch/g-C_3N_4 (Fig. 14).
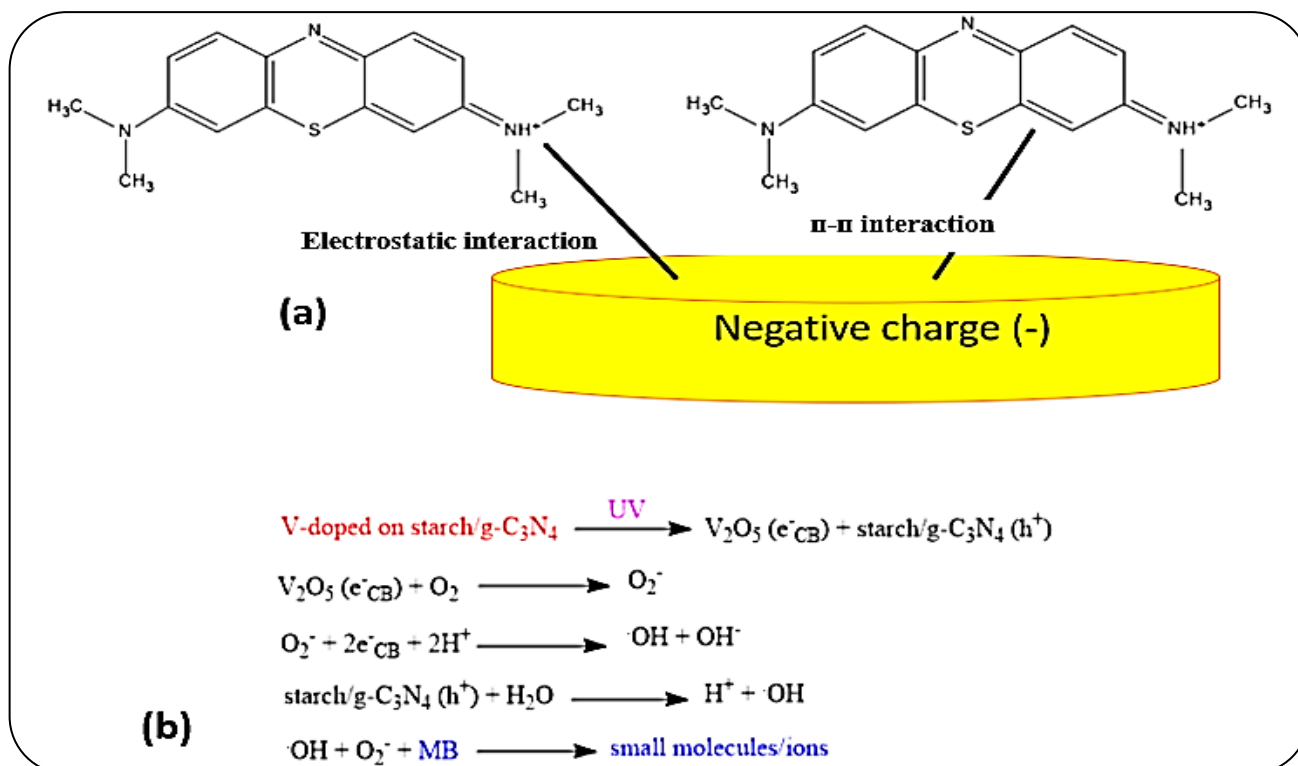
Photocatalytic study

After the adsorption process, the photocatalytic degradation was investigated at the optimum condition under dark, UV, and LED (Light-emitting Diode) irradiations. Fig. 15a shows the efficient MB removal under UV light compared to that of other conditions, because of the intensity of UV irradiation. Further, the components of composite were tested under UV conditions to illustrate the benefit of as-prepared composite. Fig. 15b shows the benefit of V-doped starch/g-C_3N_4 compared to starch and g-C_3N_4, the low separation efficiency of bare

g-C_3N_4 resulted in the decrease of photocatalytic activity. Vanadium doping as a semiconductor can extend light absorption, and the separation of electron–hole pairs was increased, so the photocatalytic activity of as-prepared composite was improved.

The mechanism of MB removal by V-doped starch/ g-C_3N_4 was studied in an aqueous solution. First, the adsorption process was performed by electrostatic and π-π interactions (Scheme 1a), then the mechanism of photocatalytic activity was explained by Scheme 1b under UV irradiation. The advantage of V-doped starch/g-C_3N_4 is the removal of MB with a high yield and eco-friendly procedure, but the decrease of BET surface can be considered as a disadvantage of the as-prepared composite, which can be studied in future research.

The adsorption cost is an important subject in efficient dye removal, thus the regeneration tests of V-doped starch/g-C_3N_4 as an adsorbent and photocatalyst

Scheme 1: Mechanism proposed by (a) adsorption and (b) photocatalytic degradation mechanism of MB by V-doped starch/g-C₃N₄ under UV irradiation.

activities were carried out. According to data, the percentage adsorption of as-prepared composite was determined four cycles of regeneration (96%, 84%, 71%, and 55%). When V-doped starch/g-C_3N_4 was applied as a photocatalyst, one cycle reusability was obtained. The reusability of photocatalyst activity was decreased, due to the production of carbon, inorganic nitrogen compounds and precipitation, and disability of the adsorbent active site.

Based on the trapping experiment results, when the scavengers were added, the yield of MB degradation was decreased, because the photocatalytic reaction was done for the MB removal. In addition, the degradation of MB was reduced from 92 % (without scavengers) to 25 %, 24.5, and 24.5 % for IPA, hydrazine, and AO, so the results showed the same role of h^+, $^{\bullet}O^{2-}$, and $^{\bullet}OH$ in photocatalytic degradation.

When the photocatalytic procedure was completed, the TOC analysis was done, and the amount of organic carbon was determined 33 ppm. The TOC removal percentage was increased to 62% after the optimum time, and it was determined that MB can be mineralized into residual organic molecules by using V-doped starch/graphitic carbon nitride.

The performance of V-doped starch/g-C_3N_4 is compared to other reported literature for determining the efficiency of as-synthesized composite. Some adsorbents reported the adsorption of MB such as carbon nanotubes [53], *Luffa cylindrica* fibers [54], graphene oxide [55], single and binary systems on wheat straw [56], and polyacrylamide/sodium alginate microsphere [57]. In these articles, the MB was transferred from the solution to another media, and the pollutant remained in the environment, because these compounds were adsorbent, and they had no ability to act as photocatalysts. The MB degradation was reported by hierarchical porous monoliths of MoO_3 nanoplates [58], polystyrene CuO/Cu_2O [59], Co-doped Ag–Au–ZnO [60], Gr/PPy modified membrane cathode [61], $Fe_3O_4/TiO_2/CuO$ [62], and $CdS@TiO_2/Ni_2P$ [63]. However, the reported photocatalyst can be applied to degrade MB, but the starting material is considered as synthetic compound, and the adsorption process and interactions of parameters weren't studied. The use of natural compounds, simple strategy, and using RSM method can be evidenced by the advantages of this work compared to other compounds.

Table 2 shows the efficiency of V-doped starch/g-C_3N_4 compared to other reported literature, which the benefit of as-synthesized composite can be seen with high yield,

Table 2: Comparison of V-doped starch/g-C$_3$N$_4$ under UV irradiation and other photocatalyst for MB removal.

Entry	Photocatalyst	Yield (%)	Condition (Irradiation type, Power, Time)	Ref
1	MFe$_2$O$_4$ (M = Co, Ni, Cu, Zn) nanoparticles	89	UV irradiation, co-precipitation-oxidation method, 8 W, 75 s	[64]
2	Multifunctional hydrogel composite based on poly(vinyl alcohol-g-acrylamide)	90	UV irradiation, UV-A ≥ 39 mW/cm^2), 16 h	[65]
3	Metalloporphyrin−Poly(vinylidene fluoride)	84	WLED, 81.7 mW cm^{-2}	[66]
4	Metal-Free g-C$_3$N$_4$	92	Xe lamp (simulated sunlight launcher with a power of 100 mW/cm^3, 120 min	[67]
5	Cobalt-doped BiVO$_4$	85	Visible-light irradiation, 150-W Xe lamp, 5h	[68]
6	Cu-doped TiO$_2$/ZnO	73.2	Visible light irradiation, 2h	[69]
7	TiO$_2$ nano-sized particles	90	UV-A light, 2h	[70]
8	V-doped on starch/g-C$_3$N$_4$	92	UV irradiation, 300-W Xe lamp, 2h	this work

by using ecofriendly compounds. Entries (1-2, 3-7) present the use of metal atoms and polymer compounds, that had shown a low yield compared to that of Entry 8. Entry 4 provides an efficient yield, but the effect and interaction of parameters weren't considered, and it was taken for 5h.

This composite can be applied to remove organic pollutants by considering important factors and can be used in real samples without effective by-products.

CONCLUSIONS

To sum up, the potential of V-doped starch/g-C$_3$N$_4$ as a novel photocatalyst was investigated to MB degradation from aqueous solution. The adsorption and photocatalytic activities of V-doped starch/g-C$_3$N$_4$ was considered for the MB removal. The RSM method based on CCD design was selected to study the main parameters including pH, MB, V-doped starch/g-C$_3$N$_4$ amounts, temperature, and time, then the interaction of parameters was obtained. The pH, MB concentration, and temperature are more effective than another parameter for the MB removal. Isotherms and kinetic models were studied for the MB adsorption by V-doped starch/g-C$_3$N$_4$ composite. The Freundlich (R^2=0.93) and pseudo-second-order (R^2=0.99) were shown the best agreement with the removal of MB process. The adsorbent can be recovered four times with no significant change in its performance, After the study of the adsorption process, the photocatalytic activity of V-doped starch/g-C$_3$N$_4$ was considered under optimum conditions (pH=8.33, 0.08 g adsorbent dose, 12 ppm of MB, 215 min, and 15 °C). After the study of photocatalytic conditions, the high percentage of MB removal was determined under UV irradiation (92 %). The findings show the application of natural compounds for the preparation of V-doped starch/g-C$_3$N$_4$ as a novel photocatalyst for MB degradation.

Recommendations for future research:

✓ Study of V-doped starch/g-C$_3$N$_4$ activity against bacteria in aqueous solution.

✓ Using the V-doped starch/g-C$_3$N$_4$ composite as a pilot in industrial wastewater.

✓ Evaluation of the as-synthesized composite for the removal of other organic pollutants.

REFERENCES

[1] Naeimi A., Nejat R., Synthesis and Characterization of a Novel Bio-Magnetically Recoverable Palladium Nanocomposite for the Photocatalytic Applications, *Iranian Journal of Chemistry and Chemical Engineering. (IJCCE),* **41(1):** 15-26 (2022).

[2] Mahmoodi N.M., Taghizadeh M., Taghizadeh A., Abdi J., Hayati B., Shekarchi A.A., Bio-Based Magnetic Metal-Organic Framework Nanocomposite: Ultrasound-Assisted Synthesis and Pollutant (Heavy Metal and Dye) Removal from Aqueous Media, *Applied Surface Science*, **480:** 288-299 (2019).

[3] Zhu Z., Huo P., Lu Z., Yan Y., Liu Z., Shi W., Li C., Dong H., Fabrication of Magnetically Recoverable Photocatalysts Using g-C$_3$N$_4$ for Effective Separation of Charge Carriers through Like-Z-Scheme Mechanism with Fe$_3$O$_4$ Mediator, *Chemical Engineering Journal,* **331:** 615-625 (2018).

[4] Osterloh F.E., Photocatalysis Versus Photosynthesis: A Sensitivity Analysis of Devices for Solar Energy Conversion and Chemical Transformations, *ACS Energy Letters*, **2:** 445-453 (2017).

[5] Singh R.S., Gautam A., Rai V., Engineering the Electronic Structure in Titanium Dioxide via Scandium Doping Based on Density Functional Theory Approach for the Photocatalysis and Photovoltaic Applications, *Iranian Journal of Chemistry and Chemical Engineering*, **42(3):** 731-739 (2022). Nazim Younes,

[6] Djamel N., Samira A., NaY Zeolite and TiO_2 Impregnated NaY Zeolite for the Adsorption and Photocatalytic Degradation of Methylene Blue under Sunlight, *Iranian Journal of Chemistry and Chemical Engineering,* **41(6):** 1907-1920 (2022).

[7] Amoresi R.A.C., Oliveira R.C., Marana N.L., de Almeida P.B., Prata P.S., Zaghete M.A., Longo E., Sambrano J.R., Simões A.Z., CeO_2 Nanoparticle Morphologies and their Corresponding Crystalline Planes for the Photocatalytic Degradation of Organic Pollutants, *ACS Applied Nano Materials*, **2:** 6513-6526 (2019).

[8] Uddin M.T., Nicolas Y., Olivier C., Toupance T., Servant L., Müller M.M., Kleebe H.-J., Ziegler J., Jaegermann W., Nanostructured SnO_2–ZnO Heterojunction Photocatalysts Showing Enhanced Photocatalytic Activity for the Degradation of Organic Dyes, *Inorganic Chemistry*, **51:** 7764-7773 (2012).

[9] Giahi M., Rahbar A., Mehdizadeh K., Photochemical Degradation of an Environmental Pollutant by Pure ZnO and MgO Doped ZnO Nanocatalysts, *Iranian Journal of Chemistry and Chemical Engineering (IJCCE)*, **40:** 83-91 (2021).

[10] Rouhi M., Babamoradi M., Hajizadeh Z., Maleki A., Maleki S.T., Design and Performance of Polypyrrole/Halloysite Nanotubes/Fe_3O_4/Ag/Co Nanocomposite for Photocatalytic Degradation of Methylene Blue under Visible Light Irradiation, *Optik*, **212:** 164721 (2020).

[11] Gnanaprakasam A.J., Sivakumar V.M., Thirumarimurugan M., Investigation of Photocatalytic Activity of Nd-Doped ZnO Nanoparticles Using Brilliant Green Dye: Synthesis and Characterization, *Iranian Journal of Chemistry and Chemical Engineering (IJCCE)*, **37(2):** 61-71 (2018).

[12] Dong G., Zhang Y., Pan Q., Qiu J., A fantastic Graphitic Carbon Nitride (g-C_3N_4) Material: Electronic Structure, Photocatalytic and Photoelectronic Properties, *Jour. Photo. Photobio. C: Photochemistry Reviews*, **20:** 33-50 (2014).l

[13] Hwang S., Lee S., Yu J.-S., Template-Directed Synthesis of Highly Ordered Nanoporous Graphitic Carbon Nitride through Polymerization of Cyanamide, *Appl. Surf. Sci.*, **253:** 5656-5659 (2007).

[14] Li X., Zhang J., Shen L., Ma Y., Lei W., Cui Q., Zou G., Preparation and Characterization of Graphitic Carbon Nitride through Pyrolysis of Melamine. *Applied Physics A*, **94:** 387-392 (2009).

[15] Denisov N., Chubenko E., Bondarenko V., Borisenko V., Synthesis of Oxygen-Doped Graphitic Carbon Nitride From Thiourea, *Technical Physics Letters*, **45:** 108-110 (2019).

[16] Zhang Y., Liu J., Wu G., Chen W., Porous Graphitic Carbon Nitride Synthesized *via* Direct Polymerization of Urea for Efficient Sunlight-Driven Photocatalytic Hydrogen Production, *Nanoscale,* **4:** 5300-5303 (2012).

[17] Zheng Y., Liu J., Liang J., Jaroniec M., Qiao S.Z., Graphitic Carbon Nitride Materials: Controllable Synthesis and Applications in Fuel Cells and Photocatalysis, *Energy & Environmental Science,* **5:** 6717-6731 (2012).

[18] Zhu J., Xiao P., Li H., Carabineiro S.A., Graphitic Carbon Nitride: Synthesis, Properties, and Applications in Catalysis, *ACS Applied Materials & Interfaces*, **6:** 16449-16465 (2014).

[19] Reddy I.N., Reddy L.V., Jayashree N., Reddy C.V., Cho M., Kim D., Shim J., Vanadium-Doped Graphitic Carbon Nitride for Multifunctional Applications: Photoelectrochemical Water Splitting and Antibacterial Activities, *Chemosphere*, **264:** 128593 (2021).

[20] Chegeni M., Mehri M., Shokri Rozbahani Z., Synthesis and Antibacterial Performance of Ag/Co_2O_3/g-C_3N_4 Nanocomposite, *Jour. Ultra. Grain. Nanostruc. Mater.*, **54(1):** 58-63 (2021).

[21] Chegeni M., Enjedani M., Graphitic Carbon Nitride Nanosheet as an Excellent Compound for the Adsorption of Calcium and Magnesium Ions: Theoretical and Experimental Studies, *Iran. J. Chem. Chem. Eng.(IJCCE)*, **41(5):** 1512-1527 (2022).

[22] Gong L., Wang X., Zhang D., Ma X., Yu S., Flexible Wearable Humidity Sensor Based on Cerium Oxide/Graphitic Carbon Nitride Nanocomposite Self-Powered by Motion-Driven Alternator and Its Application for Human Physiological Detection, *Journal of Materials Chemistry A,* **9(9):** 5619-5629 (2021).

[23] Yamsang N., Sittiwong J., Srifa P., Boekfa B., Sawangphruk M., Maihom T., Limtrakul J., First-Principle Study of Lithium Polysulfide Adsorption on Heteroatom Doped Graphitic Carbon Nitride for Lithium-Sulfur Batteries, *Applied Surface Science,* **565:** 150378 (2021).

[24] Gong L., Wang X., Zhang D., Ma X., Yu S., Flexible Wearable Humidity Sensor Based on Cerium Oxide/Graphitic Carbon Nitride Nanocomposite Self-Powered by motion-Driven Alternator and its Application for Human Physiological Detection, *Journal of Materials Chemistry A,* **9(9):** 5619-5629 (2021).

[25] Yamsang N., Sittiwong J., Srifa P., Boekfa B., Sawangphruk M., Maihom T., Limtrakul J., First-Principle Study of Lithium Polysulfide Adsorption on Heteroatom Doped Graphitic Carbon Nitride for Lithium-Sulfur Batteries, *Applied Surface Science,* **565:** 150378 (2021).

[26] Huang, Y.; Ning, L.; Feng, Z.; Ma, G.; Yang, S.; Su, Y.; Hong, Y.; Wang, H.; Peng, L.; Li, J., Graphitic Carbon Nitride Nanosheets with Low O N1-Doping Content as Efficient Photocatalysts for Organic Pollutant Degradation. *Environmental Science: Nano,* **8(2)**:460-469 (2021).

[27] Wang L., Wang C., Hu X., Xue H., Pang H., Metal/Graphitic Carbon Nitride Composites: Synthesis, Structures, and Applications, *Chemistry–An Asian Journal*, **11(23):** 3305-3328 (2016).

[28] Sun Z., Li C., Du X., Zheng S., Wang G., Facile Synthesis of Two Clay Minerals Supported Graphitic Carbon Nitride Composites as Highly Efficient Visible-Light-Driven Photocatalysts, *Journal of Colloid and Interface Science,* **511:** 268-276 (2018).

[29] Chegeni M., Mehri M., Dehdashtian S., Photocatalytic Bauxite and Red Mud/Graphitic Carbon Nitride Composites for Rhodamine B Removal, *Journal of Molecular Structure,* **1242:** 130752 (2021).

[30] Wang C., Liu G., Song K., Wang X., Wang H., Zhao N., He F., Three-Dimensional Hierarchical Porous Carbon/Graphitic Carbon Nitride Composites for Efficient Photocatalytic Hydrogen Production, *ChemCatChem*, **11(24):** 6364-6371 (2019).

[31] You S., Guo S., Zhao X., Sun M., Sun C., Su Z., Wang X., All-Inorganic Perovskite/Graphitic Carbon Nitride Composites for CO_2 Photoreduction into C1 Compounds under Low Concentrations of CO_2, *Dalton Transactions*, **48(37):** 14115-14121 (2019).

[32] Amiri M., Salehniya H., Habibi-Yangjeh A., Graphitic Carbon Nitride/Chitosan Composite for Adsorption and Electrochemical Determination of Mercury in Real Samples, *Industrial and Engineering Chemistry Research*, **55(29):** 8114-8122 (2016).

[33] Zhang C., Li Y., Shuai D., Zhang W., Niu L., Wang L., Zhang H., Visible-Light-Driven, Water-Surface-Floating Antimicrobials Developed from Graphitic Carbon Nitride and Expanded Perlite for Water Disinfection, *Chemosphere*, **208:** 84-92 (2018).

[34] Al-Azmi, A., Keshipour, S.,. Dimaval as an Efficient Ligand for Binding Ru(III) on Cross-Linked Chitosan Aerogel: Synthesis, *Characterization and Catalytic Investigation. Cellulose*, **27:** 895-904 (2020).

[35] Keshipour S., Khezerloo M., Nanocomposite of Hydrophobic Cellulose Aerogel/Graphene Quantum dot/Pd: Synthesis, Characterization, and Catalytic Application, *RSC Advances*, **9:** 17129-17136 (2019).

[36] Keshipour S., Adak K., Magnetic d-Penicillamine-Functionalized Cellulose as a New Heterogeneous Support for Cobalt(II) in Green Oxidation of Ethylbenzene to Acetophenone, *Applied Organometallic Chemistry*, **31:** e3774 (2017).

[37] Keshipour S., Ahmadi F., Seyyedi B., Chitosan-Modified Pd(II)-d-Penicillamine: Preparation, Characterization, and Catalyst Application, *Cellulose*, **24:** 1455-1462 (2017).

[38]. Al-Azmi A., Keshipour S., Cross-Linked Chitosan Aerogel Modified with Pd(II)/Phthalocyanine: Synthesis, Characterization, and Catalytic Application, *Scientific Reports*, **9**:13849 (2019).

[39] Bahluli R., Keshipour S., Microcrystalline Cellulose Modified with Fe(II)– and Ni(II)–Phthalocyanines: Syntheses, Characterizations, and Catalytic Applications, *Polyhedron*, **169:** 176-182 (2019).

[40] Fu X., Tang W., Ji L., Chen S., V_2O_5/Al_2O_3 Composite Photocatalyst: Preparation, Characterization, and the Role of Al_2O_3, *Chem. Eng. J.*, **180:** 170-177 (2012).

[41] Jiang H., Nagai M., Kobayashi K., Enhanced Photocatalytic Activity for Degradation of Methylene Blue over $V_2O_5/BiVO_4$ Composite, *Journal of Alloys and Compounds*, **479(1-2):** 821-827 (2009).

[42] Mukhtar F., Munawar T., Nadeem M.S., ur Rehman M.N., Riaz M., Iqbal F., Dual S-Scheme Heterojunction $ZnO–V_2O_5–WO_3$ Nanocomposite with Enhanced Photocatalytic and Antimicrobial Activity, *Mater. Chem. Phys.*, **263:** 124372 (2021).

[43] Oladoye P.O., Ajiboye T.O., Omotola E.O., Oyewola O.J., Methylene Blue Dye: Toxicity and Potential Elimination Technology from Wastewater, *Results in Engineering*, **16:** 100678 (2022).

[44] Iran Manesh M., Sohrabi M.R., Mortazavi Nik S., Nanoscale Zero-Valent Iron Supported on Graphene Novel Adsorbent for the Removal of Diazo Direct Red 81 from Aqueous Solution: Isotherm, Kinetics, and Thermodynamic Studies, *Iran. J. Chem. Chem. Eng. (IJCCE),* **41(6):** 1844-1855 (2022).

[45] Ali Akbari Ghavimi S., Ebrahimzadeh, M.H., Solati-Hashjin M., Abu Osman N.A., Polycaprolactone/Starch Composite: Fabrication, Structure, Properties, and Applications, *J. Biomed. Mater. Res. A*, **103(7):** 2482-98 (2015).

[46] Bagheri R., Ghaedi M., Asfaram A., Alipanahpour Dil E., Javadian H., RSM-CCD Design of Malachite Green Adsorption onto Activated Carbon with Multimodal Pore Size Distribution Prepared from Amygdalus Scoparia: Kinetic and Isotherm Studies, *Polyhedron*, **171:** 464-472 (2019).

[47] Rasoulzadeh H., Dehghani M.H., Mohammadi A.S., Karri R.R., Nabizadeh R., Nazmara S., Kim K.-H., Sahu J.N., Parametric Modelling of Pb(II) Adsorption onto Chitosan-Coated Fe_3O_4 Particles through RSM and DE Hybrid Evolutionary Optimization Framework, *Journal of Molecular Liquids*, **297:** 111893 (2020).

[48] Onu C.E., Nwabanne J.T., Ohale P.E., Asadu C.O., Comparative Analysis of RSM, ANN and ANFIS and the Mechanistic Modeling in Eriochrome Black-T Dye Adsorption Using Modified Clay, *South African Journal of Chemical Engineering*, **36:** 24-42 (2021).

[49] Naderi P., Shirani M., Semnani A., Goli A., Efficient Removal of Crystal Violet from Aqueous Solutions with Centaurea Stem as a Novel Biodegradable Bioadsorbent Using Response Surface Methodology and Simulated Annealing: Kinetic, Isotherm and Thermodynamic Studies, *Ecotoxicology and Environmental Safety*, **163:** 372-381 (2018).

[50] Abdi J., Vossoughi M., Mahmoodi N.M., Alemzadeh I., Synthesis of Amine-Modified Zeolitic Imidazolate Framework-8, Ultrasound-Assisted Dye Removal and Modeling, *Ultrasonics Sonochemistry*, **39:** 550-564 (2017).

[51] Yan S., Li Z., Zou Z., Photodegradation Performance of g-C_3N_4 Fabricated by Directly Heating Melamine. *Langmuir*, **25(17):** 10397-10401 (2009).

[52] Abdi J., Mahmoodi N.M., Vossoughi M., Alemzadeh I., Synthesis of Magnetic Metal-Organic Framework Nanocomposite (ZIF-8@SiO_2@$MnFe_2O_4$) as a Novel Adsorbent for Selective Dye Removal from Multicomponent Systems, *Microporous and Mesoporous Materials*, **273:** 177-188 (2019).

[53] Pozo C., Rodríguez-Llamazares S., Bouza R., Barral L., Castaño J., Müller N., Restrepo I., Study of the Structural Order of Native Starch Granules Using Combined FT-IR and XRD Analysis, *Journal of Polymer Research*, **25(12):** 266 (2018).

[54] Yao Y., Xu F., Chen M., Xu Z., Zhu Z., Adsorption Behavior of Methylene Blue on Carbon Nanotubes, *Bioresource Technology*, **101(9):** 3040-3046 (2010).

[55] Demir H., Top A., Balköse D., Ülkü S., Dye Adsorption Behavior of Luffa Cylindrica Fibers, *Journal of Hazardous Materials*, **153(1):** 389-394 (2008).

[56] Yan H., Tao X., Yang Z., Li K., Yang H., Li A., Cheng R., Effects of the Oxidation Degree of Graphene Oxide on the Adsorption of Methylene Blue, *Journal of Hazardous Materials*, **268:** 191-198 (2014).

[57] Zou X., Zhang H., Chen T., Li H., Meng C., Xia Y., Guo J., Preparation and Characterization of Polyacrylamide / Sodium Alginate Microspheres and its Adsorption of MB Dye, *Coll. Surf. A: Physico. Eng. Aspec.*, **567:** 184-192 (2019).

[58] Liu Y., Feng P., Wang Z., Jiao X., Akhtar F., Novel Fabrication and Enhanced Photocatalytic MB Degradation of Hierarchical Porous Monoliths of MoO_3 Nanoplates, *Scientific Reports*, **7(1):** 1845 (2017).

[59] Baghriche O., Rtimi S., Pulgarin C., Kiwi J., Polystyrene CuO/Cu_2O Uniform Films Inducing MB-Degradation under Sunlight, *Catalysis Today*, **284:** 77-83 (2017).

[60] Senthilraja A., Subash B., Krishnakumar B., Rajamanickam D., Swaminathan M., Shanthi M., Synthesis, Characterization and Catalytic Activity of co-Doped Ag–Au–ZnO for MB Dye Degradation under UV-A Light, *Materials Science in Semiconductor Processing*, **22:** 83-91 (2014).

[61] Zhao F., Liu L., Yang F., Ren N., E-Fenton Degradation of MB during Filtration with Gr/PPy Modified Membrane Cathode, *Chemical Engineering Journal*, **230**:491-498 (2013).

[62] Kianfar, A.H.; Arayesh, M.A., Synthesis, Characterization and Investigation of Photocatalytic and Catalytic Applications of $Fe_3O_4/TiO_2/CuO$ Nanoparticles for Degradation of MB and Reduction of Nitrophenols, *J. Envir. Chem. Eng.*, **8(1):** 103640 (2020).

[63] Wu K., Wu P., Zhu J., Liu C., Dong X., Wu J., Meng G., Xu K., Hou J., Liu Z., Guo X., Synthesis of Hollow Core-Shell $CdS@TiO_2/Ni_2P$ Photocatalyst for Enhancing Hydrogen Evolution and Degradation of MB, *Chemical Engineering Journal*, **360:** 221-230 (2019).

[64] Gupta N., Ghaffari Y., Kim S., Bae J., Kim K., Photocatalytic Degradation of Organic Pollutants over MFe_2O_4 (M = Co, Ni, Cu, Zn) Nanoparticles at Neutral pH. *Scientific Reports*, **10:** 4942 (2020).

[65] Kongseng P., Amornpitoksuk P., Chantarak S., Development of Multifunctional Hydrogel Composite based on Poly(Vinyl Alcohol-G-Acrylamide) for Removal and Photocatalytic Degradation of Organic Dyes, *Reactive and Functional Polymers*, **172:** 105207 (2022).

[66] Lyubimenko R., Busko D., Richards B.S., Schäfer A.I., Turshatov A., Efficient Photocatalytic Removal of Methylene Blue Using a Metalloporphyrin–Poly(vinylidene fluoride) Hybrid Membrane in a Flow-Through Reactor. *ACS Applied Materials & Interfaces*, **11(35)**:31763-31776 (2019).

[67] Xu H.-Y., Wu L.-C., Zhao H., Jin L.-G., Qi S.-Y., Synergic Effect between Adsorption and Photocatalysis of Metal-Free $g-C_3N4$ Derived from Different Precursors, **10(11):** e0142616-e0142616 (2015).

[68] Zhou B., Zhao X., Liu H., Qu J., Huang C.P., Visible-Light Sensitive Cobalt-Doped $BiVO_4$ ($Co-BiVO_4$) Photocatalytic Composites for the Degradation of Methylene Blue Dye in Dilute Aqueous Solutions, *Applied Catalysis B: Environmental*, **99(1):** 214-221 (2010).

[69] Daud W.M.A.W., Evaluating the Efficiency of Nano-Sized Cu Doped TiO_2/ZnO Photocatalyst under Visible Light Irradiation, *Journal of Molecular Liquids*, **258:** 354-365 (2018).

[70] Dariani R.S., Esmaeili A., Mortezaali A., Dehghanpour S., Photocatalytic Reaction and Degradation of Methylene Blue on TiO_2 Nano-Sized Particles, *Optik*, **127:** 7143-7154 (2016).